# Silicon-based metal-loaded plasmonic waveguides for low-loss nanofocusing

**Lucas Lafone,[1] Themistoklis P. H. Sidiropoulos,[1] and Rupert F. Oulton,[1*]**

[1]*Experimental Solid State Physics, The Blackett Laboratory, Imperial College London, London, SW7 2AZ UK*
**Corresponding author: r.oulton@imperial.ac.uk*

Received Month X, XXXX; revised Month X, XXXX; accepted Month X, XXXX; posted Month X, XXXX (Doc. ID XXXXX); published Month X, XXXX

We introduce plasmonic waveguides based on metal loading of silicon on insulator (SOI) substrates. Here slab waveguide modes hybridize with the plasmonic modes of either a metal nanowire or a slot in a metal film. By tapering a single dimension of either structure, the resulting hybrid mode can be converted from photon-like to plasmon-like allowing up to millimeter range transport and rapid nanoscale focusing down to mode areas $\sim \lambda^2/400$. Metal loading is achievable with a single lithography step directly on SOI without the need for etching and thus opens practical possibilities for silicon nanoplasmonics. 

*OCIS Codes: (240.6680) Surface plasmons, (130.2790) Guided waves (130.5990) Semiconductors, (250.5403) Plasmonics*
http://dx.doi.org/10.1364/OL.99.099999

Recent advances in nanofabrication have allowed the field of plasmonics to flourish, opening up the possibility of guiding and confining light well below the diffraction limit[1,2]. Much of the initial interest in surface plasmons surrounded the potential to reduce the size of photonic components, with many predicting wide-reaching applications[3,4]. However, to impact upon existing technologies plasmonic waveguides must combine small mode areas with manageable propagation lengths, simple deterministic fabrication techniques and compatibility with standard semiconductor materials. An adequate demonstration and analysis of a structure combining all of these characteristics is yet to be produced.

Loss is pervasive in metal optics, but semiconductor materials exacerbate the problem; propagation loss of surface plasmon polaritons (SPPs) tends to scale with $\varepsilon_r^{3/2}$, where $\varepsilon_r$ is the real part of the relative permittivity of the medium in contact with metal[2]. While loss can be inhibitive for commercially attractive semiconductors (e.g. silicon), Hybrid Plasmonic Waveguides (HPW) have become an attractive solution to the problem[2,5] despite challenges of integration with conventional photonics platforms[6,7]. Here we introduce two inverted HPWs constructed by patterning Silicon-On-Insulator (SOI) slab waveguides with metal. The approach is fascinating since the metalized regions load the underlying slab waveguide to produce a highly contrasting local mode velocity suitable for generating strong lateral mode confinement. With this lateral confinement control we explore the potential of these HPWs to efficiently transform light from long range photon-like modes into highly focused nano-scopic modes[8]. Remarkably, this approach to plasmonic waveguide taper design is fully compatible with current nano-lithography techniques and does not require silicon etching.

Cross sectional views of the two proposed waveguides are shown in Fig. 1(a). Both are hybrids of a plasmonic waveguide coupled to a silicon slab. Hybrid modes form due to the structured loading of the underlying silicon slab modes by the silver films, in a similar manner to conventional ridge waveguides. The first geometry is comprised of a silver strip sitting on a silicon slab and separated from it by an insulating spacer layer. Here, predominantly transverse magnetic (TM) modes couple to SPPs of the metal, raising the local effective index to allow guiding in the central region II. In the second structure the metallic loading guides predominantly transverse electric (TE) modes in region II, where repulsion of this electric field polarization from the metal in region I lowers the local effective index. In the following study, we examine bound modes of these HPWs using the finite element method at a wavelength of $\lambda = 1{,}550$ nm, with the silver permittivity data of Johnson & Christy[9] and silicon and silica refractive indices of 3.48 and 1.53 respectively.

For wider slots and strips the mechanism of lateral confinement can be understood by examining effective mode indices of the various lateral sections of the waveguides, labelled in Fig. 1(a) as either I or II. Treating each region separately, we calculate an effective mode index for the corresponding 1D multilayer stack. This clearly illustrates the effect of the metallic loading by the relative difference in effective indices of regions I and II, shown in Fig. 1(b). In order to support a bound mode, the effective index difference, $\Delta n_{eff} = n_{II} - n_I > 0$. Remarkably, the effective index contrast of loaded and unloaded regions can be as large as if the silicon were etched. Interestingly, the metal loading affects the two slab mode polarizations differently; SPPs hybridize with TM, but not TE slab modes. The effective index in metal loaded regions thus increases for TM, but decreases for TE modes, relative to unloaded regions. Therefore the slot supports bound TE-like modes and the strip supports bound TM-like modes.

The effective index contrast, $\Delta n_{eff}$, also depends on Si waveguide thickness, $H$, as shown in Fig. 1b). Here, we show four examples corresponding to two strip and two slot structures. The strip structures are geometrically identical expect for the refractive index of the upper half space, which controls the coupling of SPPs on either side of the metal film. The symmetric structure uses a silver strip completely embedded in silica whereas the asymmetric structure uses a silica gap region, with an air upper half space. The slot structures both use a silica upper half space but differ in the spacer width, $G$. Maximum lateral confinement, corresponding to the largest $\Delta n_{eff}$, depends on the Si thickness ($H$) and occurs near $H = 160$ nm for strip structures and $H < 100$ nm, for the slot geometries. In practice $H < 100$ nm is too thin to be compatible with silicon photonics and in subsequent simulations both structures use $H = 160$ nm.

In reality the modes of the two structures are neither pure TE nor TM, but contain all six field components with one dominating[10]. This leads to an important and rather subtle limitation: bound modes can be cut-off by coupling to either of the unbound modes of region I. A bound mode of the strip (or slot) must therefore have an effective index exceeding both TE and TM unbounded modes of region I, which thus defines critical values of spacer thickness, $G_c$. For the symmetric strip structure, there is a maximum value, $G_c \lesssim 15$ nm, while for the slot structure there is a minimum value, $G_C \gtrsim 15$ nm. This limitation was not explained in recent works describing geometries similar to the strip based structure[11], which has led to the analysis of leaky modes[12] or elaborate waveguide designs[13]. Interestingly this limitation did not apply to the original HPW of [2] as the 2D plasmonic mode of the dielectric-metal interface only supports one polarisation.

The effective index, $n_{eff}$, as a function of strip or slot width, $W$, for the various geometries is shown in Fig. 2, calculated using a 2D cross sectional finite element mode solver. The structures all exhibit similar behaviour for large values of $W$, with approximately constant $n_{eff}$. However, for small $W$, a rapid increase in effective mode index occurs for both structures due to the emergence of plasmonic characteristics. Note that the asymmetric strip structure has a cut off where the effective index of the hybrid mode drops below that of the TE mode in region I. Other reported asymmetric plasmonic waveguides similarly do not sustain bound modes for all strip widths[14].

The behaviour of the bound hybrid modes can be understood in more detail by considering the coupling between the underlying modes. The hybrid and uncoupled modes for the symmetric strip and one slot geometry ($G = 25$ nm) are shown in Fig. 3. Here we approximate these to be the plasmonic mode of a slot or strip and a photonic mode of the slab, both in uniform $SiO_2$ cladding. Since the slab waveguide only supports unbound modes, Fig. 3 shows the effective index of regions II and the largest effective index of region I that demark the limits of bound photonic mode propagation due to metallic loading (shaded area). Effective indices below these values correspond to modes not bound in 2D (cross-hatched area). Using these limits, we have estimated the momentum of a hypothetical photonic bound mode using the effective index method [15]. As expected, for thick strip or slot widths the effective indices of the hybrid modes asymptotically approach the effective index of region II, where lateral confinement is possible due to the metallic loading. Meanwhile, thin widths generate hybrid modes that approach the expected response of the underlying plasmonic modes. Between these extremities the hybrid mode effective index always exceeds those of its constituent modes due to the anti-crossing behaviour expected of coupled modes. It is noteworthy that the large mode splitting for the strip geometry indicates that mode coupling is significantly stronger than in the slot geometry.

The degree of confinement, measured by the mode area, $A_m$, and the achievable propagation length, $L_m$, are presented in the parametric plot of Fig. 4[16]. We define the mode area as,

$$A_m = \frac{\int U(\boldsymbol{r})dA}{Max\{2U_E(\boldsymbol{r})\}} \qquad (1)$$

Here, $U = U_E + U_M$ is the total electromagnetic energy density as a function of position, $\boldsymbol{r}$, and the integrations run over cross sectional areas of infinite extent perpendicular to the direction of propagation. Since the sharp corners of the metal film can exaggerate the confinement we use the maximum electric energy density along the center of the waveguides in the denominator of Eq. (1) [12]. The propagation length takes the usual definition, $L_m = 1/(2Im(\beta))$, where $\beta$ is the mode's complex propagation constant, determined directly from the mode solver. Fig. 4(a) shows that both the strip and slot geometries are capable of sustaining bound modes for all values of strip or slot widths with mode areas around two orders of magnitude smaller than the vacuum diffraction limited area, $A_0 = \lambda^2/4$. The main distinction is that for larger widths the slot geometry is capable of accessing much longer propagation distances ($> 500\lambda$). This is a highly desirable trait in a plasmonic waveguide, especially since the strong plasmonic confinement and long range photonic transport characteristics are accessible through a single geometric parameter; the slot width, $W$.

The confinement versus propagation characteristics of these geometries can be further understood with reference to the field distributions shown in Fig. 4(b-e). For small slot or strip widths, the HPW modes are predominantly plasmonic, either situated within the slot[17] or surrounding the strip[18]. For larger widths the mode of the slot geometry sits mainly in the silicon slab and is photon-like. This explains why this geometry can access long propagation distances with the intrinsic confinement of the silicon slab (Fig. 4). On the other hand, even for the widest strip structure, a large portion of energy still resides near the silver and although laterally photon-like, it maintains significant plasmonic character in the vertical dimension. Consequently, the strip geometry has an upper bound on its propagation length, which is the SPP propagation loss of unbound modes of region II.

With the appropriate choice of dimensions and cladding materials both HPW geometries allow nanofocusing simply by varying the strip or slot width. In the case of the slot structure, this provides effective mode conversion between photonic and plasmonic modes. Efficient coupling to nanoscale excitations is relevant for integrated semiconductor nano-photonics as it generates strong electric field intensities with relatively low mode powers to enhance weak non-linear effects. Nanofocusing generally requires a balance between tapering at angles large enough to avoid significant propagation losses but acute enough to mitigate scattering and reflections. Following previous works, we employ the eikonal approximation to determine an adiabatic criterion[19], where the eikonal parameter is,

$$\delta = \frac{1}{k_0}\left|\frac{d\Re(\beta(z))^{-1}}{dz}\right| \qquad (2)$$

Recent works have shown that $\delta < 1$ is sufficient for adiabatic focusing [20]. In the eikonal approximation, the enhancement factor $f(z)$, where $z$ is the distance propagated along the taper, is then given by

$$f(z) = \frac{A_{m2}(z_0)v_g(z_0)}{A_{m2}(z)v_g(z)} \exp\left\{-2k_0 \int_{z_0}^{z} \Im[\beta(s)]ds\right\} \qquad (3)$$

where $v_g(z)$ is the local group velocity of the hybrid mode. The resulting electric field enhancement associated with tapering the two geometries between $4\,\mu m < W < 20$ nm is shown in Fig. 5. The inset of Fig. 5 shows $\delta$ versus $W$. Taking 20 nm as a conservative minimum achievable slot or strip width (given current fabrication techniques), a taper angle of about $30^o$ maintains the adiabatic criterion, which eventually breaks down near the apex of the taper.

Given the ability to adiabatically focus using short tapers, propagation losses are small and the enhancement factors are primarily dependent on the change in confinement area and group velocity of the mode. For the chosen dimensions, enhancement factors of around 150 are possible with both geometries. As nonlinear effects depend on higher powers of electric field intensity, this is sufficient to significantly reduce nonlinear interaction distances in nanophotonic components.

In conclusion we have presented two plasmonic waveguides capable of low loss deep sub-wavelength energy transport and focusing using a novel metallic loading technique compatible with silicon photonics. We highlighted the physics of the approach and a number of limitations that allow for the future design and implementation of these promising structures in silicon nanophotonics applications.

## References


[1] S. Bozhevolnyi, V. Volkov, E. Devaux, and T. Ebbesen, Phys. Rev. Lett. 95, 046802 (2005).
[2] R. F. Oulton, V. J. Sorger, D. a. Genov, D. F. P. Pile, and X. Zhang, Nat. Photonics 2, 496–500 (2008).
[3] D. K. Gramotnev and S. I. Bozhevolnyi, Nat. Photonics 4, 83–91 (Nature Publishing Group, 2010).
[4] D. K. Gramotnev and S. I. Bozhevolnyi, Nat. Photonics 8, 13–22 (Nature Publishing Group, 2013).
[5] V. J. Sorger, Z. Ye, R. F. Oulton, Y. Wang, G. Bartal, X. Yin, and X. Zhang, Nat. Commun., 331–335 (Nature Publishing Group, 2011).
[6] I. Goykhman, B. Desiatov, and U. Levy, Appl. Phys. Lett. 97, 141106 (2010).
[7] V. J. Sorger, N. D. Lanzillotti-Kimura, R.-M. Ma, and X. Zhang, Nanophotonics 1, 1–6 (2012).
[8] M. Stockman, Phys. Rev. Lett. 93, 137404 (2004).
[9] P. B. Johnson and R. Christy, Phys. Rev. B 6, 4370–4379 (APS, 1972).
[10] J. D. Jackson, (Wiley, New York, NY, 1999).
[11] D. Dai and S. He, Opt. Express 17, 16646–16653 (2009).
[12] L. Gao, L. Tang, F. Hu, R. Guo, X. Wang, and Z. Zhou, Opt. Express 20, 11487–11495 (2012).
[13] Y. Bian, Z. Zheng, X. Zhao, L. Liu, Y. Su, J. Liu, J. Zhu, and T. Zhou, Phys. Status Solidi 210, 1424–1428 (2013).
[14] E. Verhagen, M. Spasenović, A. Polman, and L. Kuipers, Phys. Rev. Lett. 102, 203904 (2009).
[15] T. Tamir, (Pringer-Verlag, Berlin, 1982).
[16] R. F. Oulton, G. Bartal, D. F. P. Pile, and X. Zhang, New J. Phys. 10, 105018 (2008).
[17] G. Veronis and S. Fan, Opt. Lett. 30, 3359–3361 (2005).
[18] J. Takahara, S. Yamagishi, H. Taki, a Morimoto, and T. Kobayashi, Opt. Lett. 22, 475–477 (1997).
[19] L. D. Landau and E. M. Lifshits, in Moscow Izd. Nauk. Teor. Fiz. 8 (1982).
[20] D. K. Gramotnev, M. W. Vogel, and M. I. Stockman, J. Appl. Phys. 104, 034311 (2008).

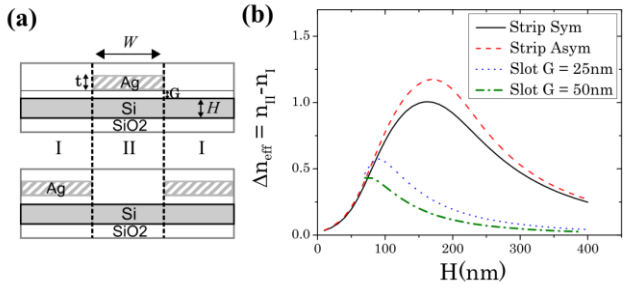


Fig. 1 a) The strip and slot geometries. $W$ is the width of slot or strip, $H$ is the thickness of the semiconductor waveguide, $G$ is the spacer thickness between the metal and slab waveguide and $t$ is the thickness of the metal. b) effective index contrast, $\Delta n_{eff}$, between regions I and II vs. $H$ for $t = 50$ nm. The strip geometries use a silica spacer with $G = 10$ nm with an upper half-space for one of silica (symmetric) and the other of air (asymmetric). The two slot geometries are embedded in silica with $G = 25$ nm and $G = 50$ nm.

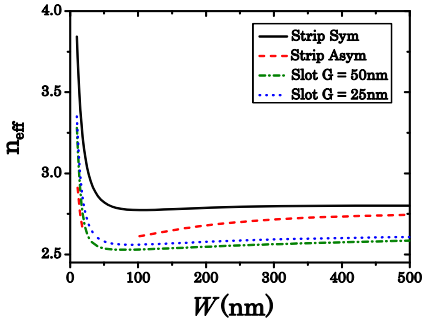


Fig. 2 Variation of effective index ($n_{eff}$) with strip width ($W$) for the same geometries shown in Fig. 1b). The break in the red dashed line, representing the asymmetric strip, is due to mode-cut off by coupling to the unbound TE mode of region I.

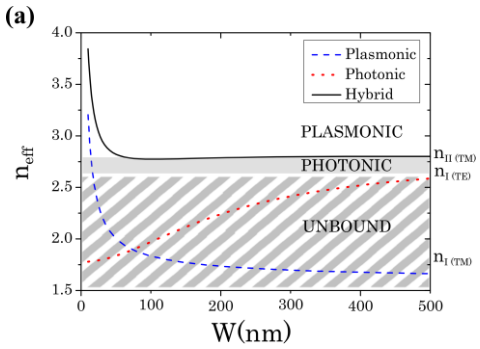


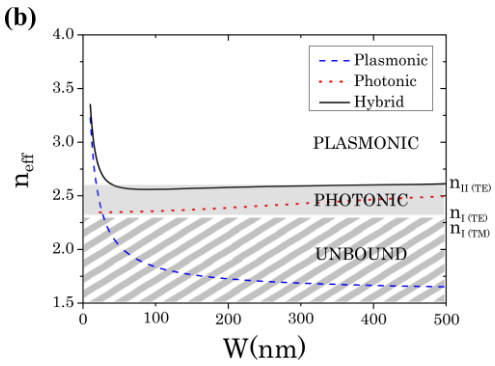


Fig. 3 Hybridization of photonic and plasmonic modes in the strip (a) and slot (b) structures, the underlying photonic and plasmonic modes outlined in the text are shown along with the resulting hybrid mode.

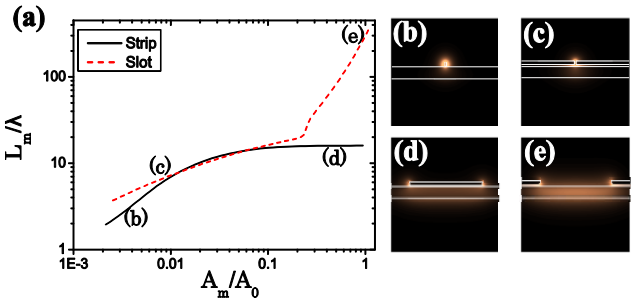


Fig. 4. (a) Parameterized plot of propagation length vs mode area. Here $H = 160$ nm and $t = 50$ nm for both slot and strip structures. Meanwhile, $G = 10$ nm for strip and 50 nm for slot. The widths of slot and strip were varied between $W = 10 - 3000$ nm. (b-e) field distributions for a 20 nm wide strip, 20 nm wide slot, 2 μm wide strip and 2 μm wide slot, respectively.

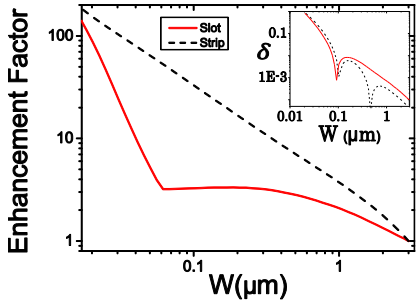


Fig. 5. Enhancement factor for the strip and slot waveguides as a function of width, W, whilst propagating along a 30° taper starting at 3μm wide and terminating at 20nm wide. Inset shows eikonal parameter for 30° taper at various widths for the chosen slot and strip.

1. Bozhevolnyi, S., Volkov, V., Devaux, E. & Ebbesen, T. Channel Plasmon-Polariton Guiding by Subwavelength Metal Grooves. *Phys. Rev. Lett.* **95,** 046802 (2005).

2. Oulton, R. F., Sorger, V. J., Genov, D. a., Pile, D. F. P. & Zhang, X. A hybrid plasmonic waveguide for subwavelength confinement and long-range propagation. *Nat. Photonics* **2,** 496–500 (2008).

3. Gramotnev, D. K. & Bozhevolnyi, S. I. Plasmonics beyond the diffraction limit. *Nat. Photonics* **4,** 83–91 (2010).

4. Gramotnev, D. K. & Bozhevolnyi, S. I. Nanofocusing of electromagnetic radiation. *Nat. Photonics* **8,** 13–22 (2013).

5. Sorger, V. J. *et al.* waveguiding at deep sub-wavelength scales. *Nat. Commun.* 331–335 (2011). doi:10.1038/ncomms1315

6. Goykhman, I., Desiatov, B. & Levy, U. Experimental demonstration of locally oxidized hybrid silicon-plasmonic waveguide. *Appl. Phys. Lett.* **97,** 141106 (2010).

7. Sorger, V. J., Lanzillotti-Kimura, N. D., Ma, R.-M. & Zhang, X. Ultra-compact silicon nanophotonic modulator with broadband response. *Nanophotonics* **1,** 1–6 (2012).

8. Stockman, M. Nanofocusing of Optical Energy in Tapered Plasmonic Waveguides. *Phys. Rev. Lett.* **93,** 137404 (2004).

9. Johnson, P. B. & Christy, R. Optical constants of the noble metals. *Phys. Rev. B* **6,** 4370–4379 (1972).

10. Jackson, J. D. *Classical Electrodynamics*. (Wiley, New York, NY, 1999).

11. Dai, D. & He, S. A silicon-based hybrid plasmonic waveguide with a metal cap for a nano-scale light confinement. *Opt. Express* **17,** 16646–53 (2009).

12. Gao, L. *et al.* Active metal strip hybrid plasmonic waveguide with low critical material gain. *Opt. Express* **20,** 11487–95 (2012).

13. Bian, Y. *et al.* Nanoscale light guiding in a silicon-based hybrid plasmonic waveguide that incorporates an inverse metal ridge. *Phys. Status Solidi* **210,** 1424–1428 (2013).

14. Verhagen, E., Spasenović, M., Polman, A. & Kuipers, L. Nanowire Plasmon Excitation by Adiabatic Mode Transformation. *Phys. Rev. Lett.* **102,** 203904 (2009).

15. Tamir, T. *Topics in applied physics vol 7 Integrated Optics*. (Springer-Verlag, 1982).

16. Oulton, R. F., Bartal, G., Pile, D. F. P. & Zhang, X. Confinement and propagation characteristics of subwavelength plasmonic modes. *New J. Phys.* **10,** 105018 (2008).

17. Veronis, G. & Fan, S. Guided subwavelength plasmonic mode supported by a slot in a thin metal film. *Opt. Lett.* **30,** 3359–61 (2005).

18. Takahara, J., Yamagishi, S., Taki, H., Morimoto, a & Kobayashi, T. Guiding of a one-dimensional optical beam with nanometer diameter. *Opt. Lett.* **22,** 475–7 (1997).

19. Landau, L. D. & Lifshits, E. M. *The electrodynamics of continuous media. Moscow Izd. Nauk. Teor. Fiz.* **8,** (1982).

20. Gramotnev, D. K., Vogel, M. W. & Stockman, M. I. Optimized nonadiabatic nanofocusing of plasmons by tapered metal rods. *J. Appl. Phys.* **104,** 034311 (2008).